

Effects of iron limitation on the expression of metabolic genes in the marine cyanobacterium *Trichodesmium erythraeum* IMS101

Tuo Shi,^{1†} Yi Sun² and Paul G. Falkowski^{1,3*}

¹*Environmental Biophysics and Molecular Ecology Program, Institute of Marine and Coastal Sciences, Rutgers University, New Brunswick, NJ 08901, USA.*

²*Department of Molecular Biology and Biochemistry, Waksman Institute of Microbiology, and* ³*Department of Geological Sciences, Rutgers University, Piscataway, NJ 08854, USA.*

Summary

Iron deficiency in axenic cultures of *Trichodesmium erythraeum* IMS101 led to significant declines in both nitrogen fixation rates and photochemical energy conversion efficiency, accompanied by downregulation of genes encoding the major iron-binding proteins, including *psbA* and *psbE* of photosystem II, *psaA* and *psaC* of photosystem I, *petB* and *petC* of the cytochrome *b₆f* complex, and *nifH*. However, the iron-starved cultures remained viable and expression of the metalloprotein genes was partially or fully restored within 3 days following the addition of iron. Both physiological and molecular responses revealed that expression and synthesis of the nitrogen fixation and photosynthetic machinery follow the hierarchy of iron demand; that is, nitrogen fixation was far more susceptible to iron limitation than photosynthesis. Consequently, the *nifH* transcript exhibited a 1–2 day shorter half-life and two to three times faster degradation rate than that of the photosynthetic genes. Our results suggest that the changes in gene expression are related to the redox state in the shared photosynthetic/respiratory pathway which, when faced with short-term iron deficiency, signals *Trichodesmium* to selectively sacrifice nitrogen fixation to conserve iron for photosynthetic and respiratory electron transport. The observed functional and compositional alterations represent the compromises in gene expression and acclimation capacity between

two basic metabolic pathways competing for iron when it is limiting.

Introduction

Oceanic nitrogen fixation provides an important source of 'new' nitrogen to sustain the net carbon fixation and export of organic matter from the euphotic zone (Karl *et al.*, 1997), and potentially limits global primary productivity on geological timescales (Falkowski, 1997). In the contemporary ocean, a large fraction of nitrogen fixation appears to be accomplished by filamentous, non-heterocystous cyanobacteria in the genus *Trichodesmium* that inhabit tropical and subtropical surface waters (Capone *et al.*, 1997; Davis and McGillicuddy, 2006; Westberry and Siegel, 2006). However, despite the potential selective advantage of nitrogen fixation in nitrogen-limited areas of the ocean, only a few species of *Trichodesmium* (Carpenter, 1983; Lundgren *et al.*, 2005) and other unicellular non-heterocystous diazotrophic cyanobacterial species (Zehr *et al.*, 2001) have been identified in the open ocean. Moreover, natural blooms of *Trichodesmium* in oligotrophic ocean are often observed to terminate abruptly by unknown mechanisms. Hence, there must be strong selection pressures limiting the abundance and radiation of marine cyanobacteria in world's ocean.

Iron (Fe) is an absolutely required redox component for virtually all organisms and may have catalysed reactions that constitute the first steps in the origin of life (Cody *et al.*, 2000). Iron is also a key element for the synthesis of several cellular compounds, e.g. ribonucleotides, haem and chromophores (Straus, 1994). Compared with heterotrophs, obligate photosynthetic diazotrophs, including *Trichodesmium*, have an additional need for iron due to the abundance of iron-containing enzymes in both their photosynthetic and nitrogen fixation apparatus (see Table 1). Thus, the availability of iron is critically important in determining the regulation and function of photosynthetic and diazotrophic growth. Although iron is the most abundant transition element in the Earth's crust, the exceedingly low solubility (10^{-18} M) of the dominant iron form (Fe^{3+}) in aerobic ecosystems (Braun *et al.*, 1990), coupled with the fact that the major source of iron flux to the open ocean gyres is from atmospheric dust deposition

Received 28 March, 2007; accepted 16 June, 2007. *For correspondence. E-mail falko@marine.rutgers.edu; Tel. (+1) 732 932 6555 ext. 370; Fax (+1) 732 932 4083. †Present address: Department of Ocean Sciences, University of California, Santa Cruz, 1156 High Street, Santa Cruz, CA 95064, USA.

Table 1. Fe components of the electron transport chains of nitrogen fixation and photosynthetic apparatus.

Complex	Fe-containing cofactor ^a	Number of Fe atoms ^b	Fe-binding protein	Gene
Nitrogenase complex		19		
Nitrogenase reductase	1 [4Fe-4S]	4	Fe protein	<i>nifH</i>
Nitrogenase	1 P cluster ([8Fe-7S])	8	MoFe protein α/β -subunits	<i>nifD/K</i>
	1 FeMoCo ([7Fe-9S-Mo])	7		
Photosynthetic apparatus		~23–24		
PSII		3		
	1 non-haem iron	1	D1/D2	<i>psbA/psbD</i>
	1 haem	1	Cyt <i>b</i> ₅₅₉ α/β -subunit	<i>psbE/F</i>
	1 haem	1	Cyt <i>c</i> ₅₅₀	<i>psbV</i>
Cyt <i>b</i>₆<i>f</i> complex		6		
	3 haems	3	Cyt <i>b</i> ₆	<i>petB</i>
	1 haem	1	Cyt <i>f</i>	<i>petA</i>
	1 [2Fe-2S]	2	Rieske iron-sulfur protein	<i>petC</i>
PSI		12		
	1 F _X ([4Fe-4S])	4	Iron-sulfur protein	<i>psaC</i>
	1 F _A ([4Fe-4S])	4		
	1 F _B ([4Fe-4S])	4		
Other		3		
Cyt <i>c</i> ₅₅₃	1 haem	1	Cyt <i>c</i> ₅₅₃	
Ferredoxin	1 [2Fe-2S] centre	2	Ferredoxin	<i>petF</i>

a. Based on documented crystal structures of nitrogenase complex and photosystems (Schindelin *et al.*, 1997; Jordan *et al.*, 2001; Kurisu *et al.*, 2003; Ferreira *et al.*, 2004).

b. Numbers in bold indicate total number of iron atoms per monomer.

(Duce and Tindale, 1991; Gao *et al.*, 2001), severely restricts the availability of this key element for marine photoautotrophs over large areas. The paucity of iron in the surface ocean has led to the hypothesis that iron limits primary productivity and phytoplankton growth in the vast, otherwise high-nutrient regions of the world's oceans (Martin *et al.*, 1994; Behrenfeld *et al.*, 1996; 2006; Boyd *et al.*, 2007).

The impacts of iron on growth, C and N fixation, O₂ production and dark respiration in *Trichodesmium* have been established by direct experimental manipulation of iron concentrations in cultures (Rueter *et al.*, 1990; Paerl, 1994; Berman-Frank *et al.*, 2001a). The observed and theoretical iron requirements and iron use efficiency were measured in marine phytoplankton in general (Raven, 1990; Morel *et al.*, 1991; Rueter *et al.*, 1992) and have been revised for *Trichodesmium* specifically (Kustka *et al.*, 2003a). Moreover, the relationship between cellular iron quotas and growth response has been quantified (Berman-Frank *et al.*, 2001a; Kustka *et al.*, 2003b). However, relatively little is known of the molecular responses of *Trichodesmium* to iron stress. Webb and colleagues (2001) demonstrated that iron stress in cultured marine cyanobacteria, including *Synechococcus* spp., *Crocospaera* sp. and *Trichodesmium* sp., induced specific proteins, such as IdiA (Michel *et al.*, 1996), possibly for cellular iron scavenging. However, no molecular study has, to date, focused specifically on whole cell metabolic gene expression and regulation in response to iron limitation in any marine cyanobacterium.

Here we report on the physiological and molecular responses of both the photosynthetic and the nitrogen-

fixing machineries to iron bioavailability in axenic cultures of *Trichodesmium erythraeum* IMS 101. Our primary goals are to understand the molecular basis for the iron deficiency in the two metabolic pathways and to elucidate how iron reconstitution restores metabolic functions.

Results

Physiological characteristics in Fe-limited Trichodesmium

Trichodesmium cells exhibited characteristic phenotypic changes when transferred to Fe-deficient media. Compared with Fe-sufficient (+Fe) control, Fe-deficient (–Fe) cultures grew at reduced rates and to lower final cell densities (Fig. 1A). The reduced biomass was accompanied by a decrease in cell chlorophyll accumulation, a hallmark of Fe deficiency in cyanobacteria (Öquist, 1974). The chlorophyll accumulation of Fe-deficient cells was indistinguishable from the control during the first 24 h of growth, but began to slow down after day 2, and dropped to below 50% of Fe-sufficient levels after 6 days of starvation (Fig. 1B). The room-temperature optical absorption spectrum of Fe-deficient cells had a ~5 nm blue shift in the chlorophyll absorption band, compared with that of Fe-sufficient control (Fig. 1C). Low temperature fluorescence emission spectra resolved characteristic peaks associated with photosystem II (PSII) core antenna complexes (685 and 695 nm), and photosystem I (PSI) chlorophyll–protein complex (715 nm) (Fig. 1D). We observed an increase in the relative amplitude of the 685 nm peak and a decrease of the PSI associated peak

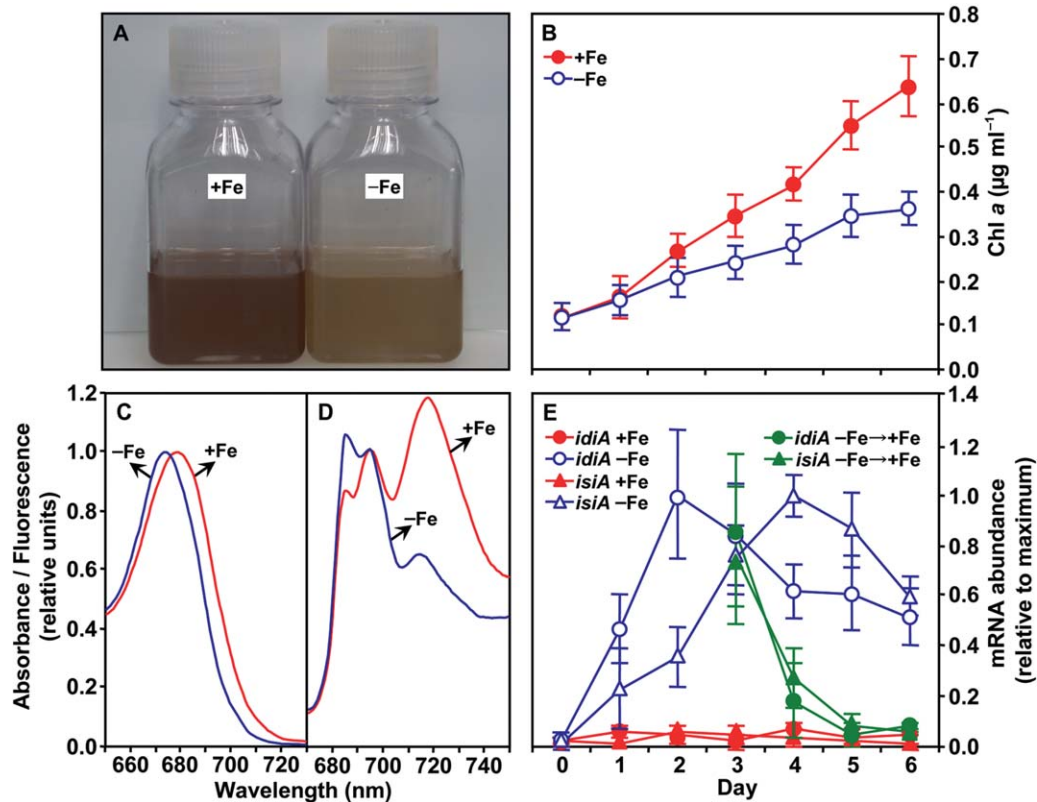


Fig. 1. Characteristics of *Trichodesmium erythraeum* IMS101 corresponding to Fe limitation.

A. Cultures grown in YBCII media with Fe supplemented (+Fe) or depleted (-Fe) at 26°C for 6 days on a 12:12 h light/dark cycle under 100 $\mu\text{mol quanta m}^{-2} \text{s}^{-1}$. Fe stress was visually assessed by reduced biomass and pigmentation relative to Fe-sufficient control.

B. Chlorophyll concentration of Fe-sufficient and Fe-deficient cultures with the same initial density. Values were averages from three independent experiments and error bars indicate one standard deviation.

C. Room-temperature absorption spectra of cultures after 4 days of growth in Fe-sufficient (red line) or Fe-deficient (blue line) media showing the chlorophyll absorption maximum. The blue shift of the chlorophyll absorption peak at ~ 674 nm is typical for cells expressing *IsiA* under iron starvation. The absorption spectra were averages of six measurements from three independent experiments and normalized to the chlorophyll peak to aid comparison.

D. Low-temperature (77K) fluorescence emission spectra of cells after 4 days of growth in Fe-sufficient (red line) or Fe-deficient (blue line) media. Fluorescence emission peaks centred at 685 nm, 695 nm and 715 nm are assigned to the chlorophyll-protein complexes of the PSII antenna, the PSII and PSI core complexes, respectively. The fluorescence spectra were averages of four to six corrected scans from three independent experiments and were normalized to the peak centred at 695 nm. Chlorophyll fluorescence was excited at 435 nm.

E. Expression of iron stress signature genes *idiA* (circle) and *isiA* (triangle) in cells shifted from Fe-sufficient (red) to Fe-deficient (blue), or from Fe-deficient (blue) to Fe-replenished (green) conditions. Gene expression was induced and enhanced during the early phase of Fe limitation. In contrast, Fe replenishment downregulated transcription of iron stress related genes. Transcript abundances were normalized to the maximal values. Error bars indicate the standard deviation from three independent experiments.

at 720 nm when Fe-sufficient cells were shifted to Fe-deficient media. Both the blue shift, long-wavelength chlorophyll *a* absorption maximum and the dominant 77K emission peak at 685 nm are indicative of the induction of the *isiA* gene product, *IsiA* (also called CP43') (Öquist, 1974; Burnap *et al.*, 1993; Straus, 1994), which is homologous to PsbC, the CP43 protein of PSII.

We used the two iron-regulated genes, *idiA* and *isiA*, as markers for the Fe nutritional status of the culture. Both genes were induced after 24 h of growth in Fe-deficient media; the expression of *idiA* reached a maximum on day 2, while *isiA* mRNA reached its maximum on day 4 (Fig. 1E). This resulted in a 50-fold increase in transcript level compared with that in the Fe-sufficient control, and

the elevated expression was maintained throughout the later phase of Fe limitation. In Fe-replenished cultures, however, the release from Fe starvation led to a rapid decline in transcript level of *idiA* and *isiA* genes, which reached the control value within 24 h.

Iron-responsive nitrogen fixation rate and photochemical efficiency

We monitored the development of Fe deficiency in *Trichodesmium* IMS 101 for 6 days after the exponential-phase cultures were transferred to fresh media lacking Fe. To demonstrate the ability of cells to recover from short-term iron deficiency, iron was supplemented to the

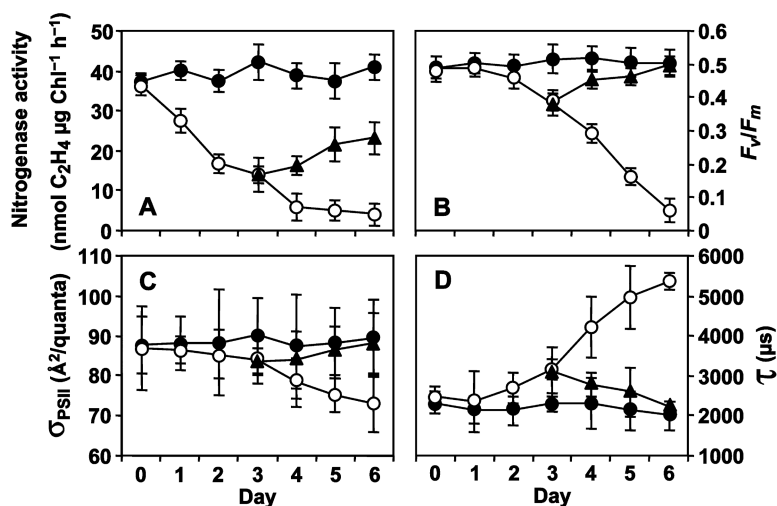


Fig. 2. Characteristics of nitrogen fixation and photosynthesis, as measured by acetylene reduction rate and fast repetition rate fluorescence (FRRF), respectively, in *Trichodesmium* sp. IMS101 cells that were grown in Fe-sufficient (filled circle) control, Fe-deficient (open circle) or a shift from Fe-deficient to Fe-sufficient (filled triangle) conditions. See details of experimental manipulations in *Experimental procedures*. The cultures were monitored every 24 h during a 6-day growth period. The nitrogenase activity (A), photosystem II (PSII) photochemical conversion efficiency (F_v/F_m , B) and functional absorption cross section (σ_{PSII} , C), and the redox state of Q_A^- (τ , D) were determined. Mean values \pm SD were calculated from a total of eight measurements from four independent experiments.

Fe-omitted culture immediately upon the observation of reduced biomass and pigmentation, which typically occurred between days 3 and 4. We then measured the effects of iron on nitrogen fixation and photosynthesis under these three different iron regimes (sufficient, deficient and replenished), as described.

Nitrogenase activity remained constant for Fe-sufficient cultures, but was significantly reduced in Fe-deficient cells (Fig. 2A). The exposure of *Trichodesmium* cells to low iron immediately led to a reduction in nitrogen fixation efficiency that decreased to about 30% of the levels in iron-sufficient cells by day 3. This was followed by a gradual decrease of nitrogenase activity to ~15% after 6 days of Fe deficiency. However, nitrogenase activity started to increase within 24 h after Fe was amended to Fe-deficient cultures, and reached up to 65% of Fe-sufficient level after 3 days of reconstitution (Fig. 2A).

In contrast to the rapid decline of nitrogen fixation capacity, iron-limited *Trichodesmium* retained relatively high photochemical energy conversion efficiency of PSII during the first 2 days of growth (Fig. 2B). However, PSII quantum yield dropped to 80% on day 3, followed by a further steady decline, and at the last time point (6 days) it had dropped to 15% compared with the initial value observed in Fe-sufficient cells (Fig. 2B). Fe-deficient cells had slightly smaller functional absorption cross-section of PSII, compared with iron-sufficient cells (Fig. 2C). This change implies a decline in the antenna size, probably due to the decomposition of phycobilisomes. The Q_A^- reoxidation rate declined significantly following 2 days of Fe deficiency, suggesting that the electron transfer components on the acceptor side of PSII [e.g. at the plastoquinone (PQ) pool] are chemically reduced (Fig. 2D). Both the PSII photochemical efficiency and Q_A^- reoxidation rate recovered rapidly (within a day) and reached a level comparable to the control after 3 days of Fe restoration (Fig. 2B and D).

Transcriptional regulation of nitrogen-fixing and photosynthetic genes

Using real-time quantitative reverse transcription polymerase chain reaction (RT-PCR), we measured the abundance of transcripts of genes encoding chlorophyll-, haem- and iron-containing protein constituents in nitrogen fixation and the photosynthetic apparatus during the transition from Fe-sufficient to Fe-limited growth, and from Fe-deficient to Fe-replenished condition. Transcript levels of *nifH* remained constant in Fe-sufficient cells over the entire experiment period; whereas they declined sharply to roughly 20% of the initial level after 3 days of Fe deprivation and became almost undetectable after 6 days of prolonged Fe deficiency (Fig. 3A). In contrast, transcript levels of *nifH* began to increase 24 h after iron was replenished to Fe-deficient cells and reached ~50% the level that in Fe-sufficient cultures at the end of the time-course. Moreover, nitrogenase activity (Fig. 2A) closely tracked the *nifH* transcript abundance (Fig. 3A).

Transcript levels of all the measured photosynthetic genes displayed a fundamentally similar pattern; that is, a steady or eventually increased gene expression until the end of the experiment for Fe-sufficient cells, but substantial decline after 2 days of transition to the Fe-deficient media, and resulted in < 10% level of the observed Fe-sufficient control. In contrast to the transcript reduction in Fe-deficient cells, a steady increase in the expression of these photosynthetic genes in the Fe-replenished cells was observed, which ultimately resulted in a comparable level of transcripts as those measured in Fe-sufficient cultures by the end of growth period (Fig. 3B–H).

Differential gene expression in different systems

Differential gene expression between nitrogen fixation and photosynthesis is even more pronounced when transcript abundance in Fe-deficient cells was normalized

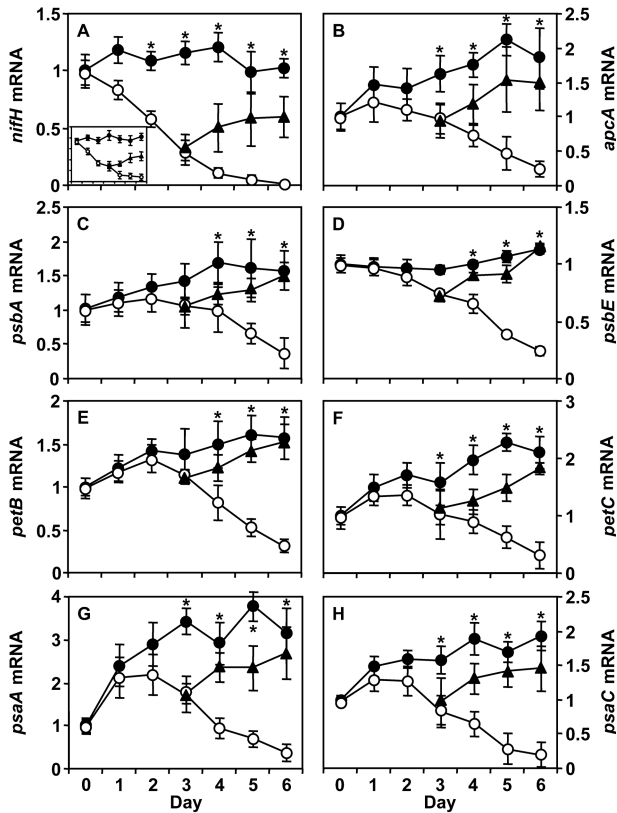


Fig. 3. Time-course showing expression of genes encoding the core components of nitrogen fixation and photosynthetic apparatus, which utilize iron as a cofactor, in different iron regimes as shown in Fig. 2. The relative change in gene expression was endogenously normalized to the housekeeping gene *mpb* using the $2^{-\Delta\Delta Ct}$ method (Livak and Schmittgen, 2001) with the ΔCt ($Ct_{\text{target}} - Ct_{\text{mpb}}$) of the time zero Fe-sufficient control used as the calibrator. Error bars indicate standard deviation from two to three independent experiments. Insert: nitrogenase activity as shown in Fig. 2. * $P < 0.05$, +Fe versus -Fe.

to the Fe-sufficient control at each time point (Fig. 4). In general, all the measured genes exhibited steady declines in transcript abundance throughout the entire period, but *nifH* declined to a much greater extent than genes encoding the photosynthetic apparatus ($P < 0.05$). For example, *nifH* transcripts exhibited the fastest degradation rate (1.1 day^{-1}) and the shortest effective transcript

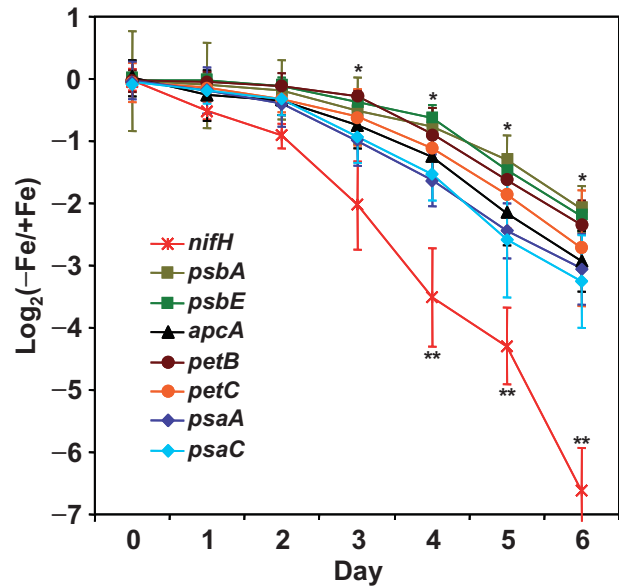


Fig. 4. Differential display in expression of nitrogen fixation and photosynthetic genes during the time-course of Fe deprivation. The extent of regulation was demonstrated by plotting with the ratios of mRNA abundance in Fe-deficient to Fe-sufficient cells. Differential expression is pronounced between *nifH* and other photosynthetic genes, and can be broadly divided into three groups based on the extent to which gene is downregulated. PSI is downregulated to a greater extent than PSII and Cyt *b_{6f}*, whereas nitrogen fixation is the most downregulated. Error bars indicate standard deviation from two to three independent experiments. * $P < 0.05$, *psaA/psaC* versus *psbA/psbE*; ** $P < 0.01$, *nifH* versus others.

half-life of ~ 2.5 days (Table 2), suggesting that nitrogen fixation is far more sensitive to Fe stress than photosynthesis. PSII appears to be less sensitive to Fe limitation than PSI, as the half-lives of *psaA* and *psaC* transcripts are $\sim 70\%$ that of *psbA* and *psbE*. The extent to which the photosynthetic genes were downregulated appeared to follow a hierarchy of PSI > cytochrome (Cyt) *b_{6f}* > PSII (Fig. 4 and Table 2).

Discussion

Our experimental results reveal that, when faced with short-term Fe deficiency, *Trichodesmium* IMS 101 employs a strategic shift in metabolic gene expression to conserve

Table 2. Apparent half-lives, effective degradation rates and effective recovery rates of photosynthesis and nitrogen-fixation gene transcripts.

Gene	Apparent half-life (day)	Effective degradation rate (day^{-1})	Effective recovery rate (day^{-1})
<i>nifH</i>	2.54**	-1.07**	0.09**
<i>psaA</i>	3.53*	-0.53*	0.18
<i>psaC</i>	3.52*	-0.56*	0.16
<i>apcA</i>	3.79	-0.49	0.15
<i>petB</i>	4.61	-0.39	0.14
<i>petC</i>	4.05	-0.44	0.22
<i>psbA</i>	4.89*	-0.33*	0.12
<i>psbE</i>	4.86*	-0.36*	0.13

* $P < 0.05$, *psaA/psaC* versus *psbA/psbE*; ** $P < 0.01$ *nifH* versus others.

Fe for photosynthetic and respiratory electron transport at the expense of nitrogen fixation. As obligate photosynthetic diazotrophs, *Trichodesmium* spp. require the synthesis of the photosynthetic apparatus (components of which also are required for respiratory electron transport), and nitrogen-fixing machinery. In all cyanobacteria, the functional photosynthetic apparatus requires 23–24 Fe atoms, depending on whether Cyt *c₅₅₃* or plastocyanin is used as an electron donor to PSI (Table 1; Ferreira and Straus, 1994). To function effectively, the core components of PSII, Cyt *b_{6f}* and PSI require highly coordinated protein–protein and protein–cofactor interactions (Shi *et al.*, 2005). Moreover, nitrogenase itself contains up to 19 iron atoms per heterodimeric protein complex moiety, and has the lowest iron use efficiency of any iron-containing enzyme involved in nitrogen metabolism (Table 1; Raven, 1988). Hence, the availability of iron appears to be a critical factor in regulating the differential expression and function of photoautotrophic and diazotrophic growth.

Although iron deficiency leads to significant declines in both nitrogen fixation and photochemical efficiency, Fe-limited *Trichodesmium* selectively sacrifices nitrogenase. The sacrifice is accomplished at both the transcriptional and post-translational levels (Figs 2 and 3). In iron-sufficient cells, the average half-life of *nifH* transcripts in *Trichodesmium* is on the order of ~2 h and is controlled by a circadian clock (Chen *et al.*, 1998). The holoenzyme is synthesized *de novo* at the start of the photoperiod, reaching a maximum during mid-day, and degraded during second half of the photoperiod and throughout the scotophase by an as yet unidentified signal transduction pathway. Under Fe-deficient conditions, however, it appears that not only is nitrogenase activity lost, but transcript levels are greatly attenuated (Figs 2 and 3). The regulatory feedback between Fe availability and *nifH* transcription is unknown. While there may be a specific Fe binding site in the promoter region of the *nif* operon, i.e. an Fe-dependent regulator mediating *nifH* transcription in a similar manner to the iron-stress-response genes (Ghassemian and Straus, 1996; Yousef *et al.*, 2003), an alternative signal is highly possible. The rapid decline in nitrogenase activity effectively removes a sink for both reductant and energy that would otherwise be supplied by respiratory electron flow through the Cyt *b_{6f}* complex. This complex also energetically couples PSII to PSI in cyanobacteria by oxidizing the plastoquinone pool. Hence, we propose that Fe-limited cells growing in the light are 'over-reduced'; that is, without sufficient sinks, electrons generated photochemically in PSII from the oxidation of water and those emanating from the oxidation of organic carbon via respiration create a 'traffic jam' at the Cyt *b_{6f}* complex (Fig. 5). This results in a highly reduced plastoquinone pool. This prediction is supported by the significantly lower F_v/F_m values

in Fe-limited cells, and longer turnover times on the acceptor side of PSII (Fig. 2B and D).

The 'Fe-over reduction' hypothesis leads to some, perhaps counter-intuitive, corollaries. Over-reduction of the plastoquinone pool downregulates the expression of photosynthetic electron transport genes (Escoubas *et al.*, 1995; Durnford and Falkowski, 1997). In effect, Fe-limited cells acquire a phenotype similar to cells exposed to high light: they have reduced antenna sizes (lower phycobilisome levels) (Guikema and Sherman, 1983; Pakrasi *et al.*, 1985) and a lower abundance of reaction centres and electron transport components (Greene *et al.*, 1991; Geider and La Roche, 1994). This phenomenon reduces electron flow through the photosynthetic electron transport chain: a negative feedback. To disperse the congestion of electron flow, *Trichodesmium* cells appear to synthesize an additional antenna ring of IsiA molecules around the fewer remaining PSI centres under conditions of iron stress in a similar manner to other well-characterized cyanobacteria (Bibby *et al.*, 2001; Boekema *et al.*, 2001). The relatively small increase in emission at 685 nm (Fig. 1), relative to the amount of *isiA* gene expression, provides evidence that this protein is reasonably well coupled to PSI. It should be noted, however, that this is not exactly the same as a high light response, which apparently does not require a large antenna for both photosystems. While it is not clear whether this extra ring of chlorophyll-binding proteins may function to protect the photosystems from photoinhibition or oxidative stress (Park *et al.*, 1999; Sandström *et al.*, 2002), it helps alleviate the over-reduction of the plastoquinone pool. On the other hand, the degradation of nitrogenase and secondarily PSI, both of which have a much higher demand for Fe (Table 1), potentially allows Fe from both complexes to be scavenged and recycled for the synthesis and repair of proteins in the photosynthetic/respiratory electron transport chain, while the degradation of phycobilisomes and other protein complexes (e.g. RuBisCO) potentially provides amino acids. These two scavenging pathways are critical for maintaining basal metabolic energy for the cells at the expense of the growth of new cells. In effect, the response to Fe depletion is to metabolically 'hibernate' until a pulse of iron allows the cell to rapidly upregulate the basic metabolic pathways, and synthesize nitrogenase and key components of the photosynthetic and respiratory electron transport chain to acquire C, N and other essential elements for cell growth. The restoration is demonstrated in experiments where Fe is replenished to Fe-deficient cells; gene expression is upregulated and becomes almost indistinguishable from the Fe-sufficient cells (Fig. 3). It should be noted, however, that in severely deficient cells (after 6 days of Fe-depletion) when growth is almost completely arrested it took ~2 weeks for the cells to fully recover (data not shown). This recovery may be

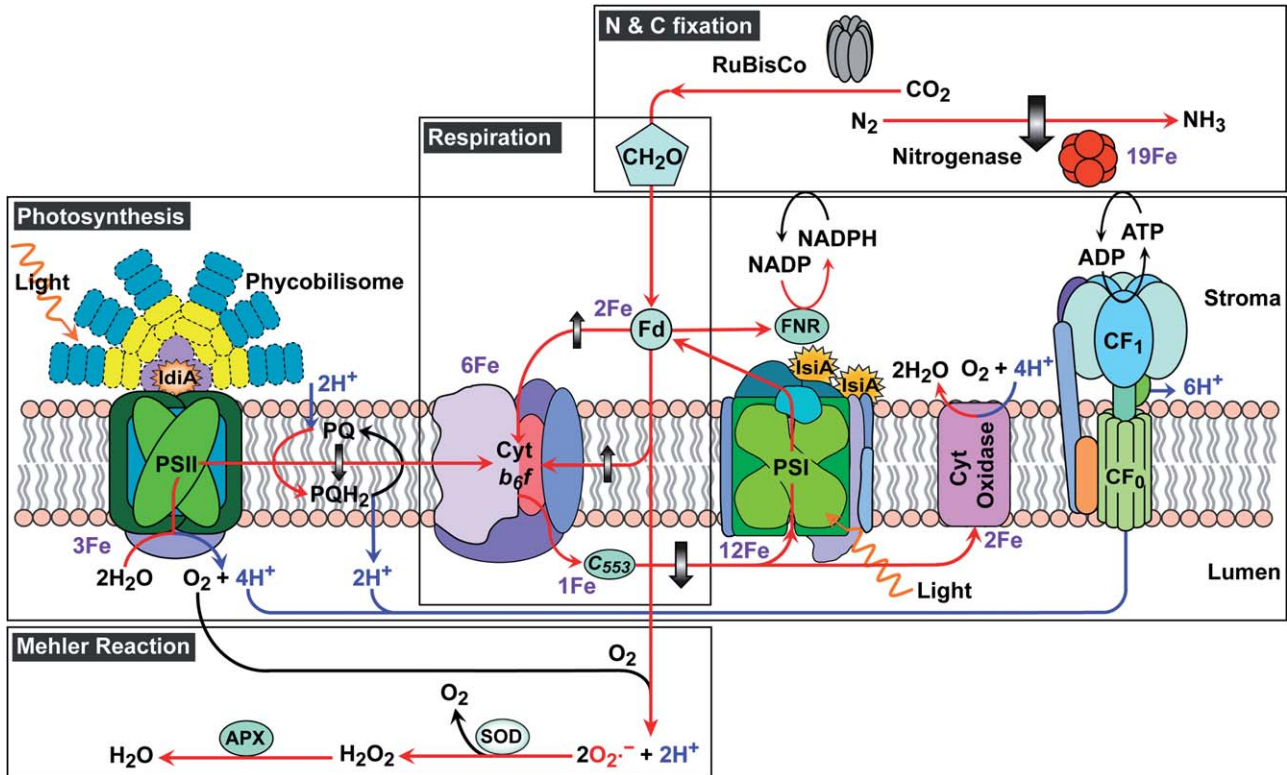


Fig. 5. Schematic model illustrating the effects of iron limitation on the rates of the electron transport among primary components in photosynthesis, nitrogen fixation, respiration and Mehler reaction pathways in *Trichodesmium erythraeum* IMS 101. Iron deficiency triggers the synthesis of IsiA forming an additional antenna around PSI (Bibby *et al.*, 2001; Boekema *et al.*, 2001), and the expression of IdiA protein, which has an implicit role in protecting the acceptor side of PSII to compensate for phycobilisome degradation (dashed contour) (Michel and Pistorius, 2004; Lax *et al.*, 2007). The block arrows indicate the hierarchical decreases in linear electron transport from PSII to Cyt b_{6f} to PSI and finally to nitrogenase (see text), the increase in cyclic electron transport around PSI, and the increase in respiratory electron transport (Ivanov *et al.*, 2000; Yousef *et al.*, 2003; Michel and Pistorius, 2004), which together lead to the over-reduction of the plastoquinone pool (PQ, PQH₂). The over-reduction hypothesis is supported by the hierarchically repressed gene expressions and activities of the representative metalloprotein complexes (Figs 2 and 4), the extent of which is in proportion to Fe requirement for each respective component (purple text and Table 1). This in turn leads to an increased production of reactive oxygen species (ROS), potentially compromising the oxygen consumption by Mehler reaction as several ROS-detoxifying enzymes such as superoxide dismutase (SOD) and ascorbate peroxidase (APX) require Fe as a cofactor. Red arrows, electron transport; blue arrows, proton transport.

slowed within the population by stress-induced autocatalysed cell death (Berman-Frank *et al.*, 2004). Hence, in regions of the upper ocean that are chronically deprived of Aeolian iron (such as the South Pacific), *Trichodesmium* may not respond rapidly to pulses of Fe (there would potentially be a long lag time between the addition of the metal and the growth of the organism). This behaviour is in strong contrast to non-nitrogen-fixing cyanobacteria. *Synechococcus* sp. PCC 7942 remains viable after 9 days of Fe starvation, but is indistinguishable from control cells after only 24 h following iron addition (Sandström *et al.*, 2002). The contrast suggests that diazotrophy imposes additional demands beyond those attributed to photosynthesis and respiration, namely, lower overall rates of transcription, protein synthesis and growth.

Both physiological and molecular responses reveal that *Trichodesmium* tends to follow the hierarchy of Fe demand to regulate the expression and synthesis of nitrogen fixa-

tion and photosynthesis. The more Fe is required, the more the system is suppressed by Fe stress. Nitrogenase complex requires the highest number of iron atoms among the competitive metabolic pathways, and thus is affected most by Fe limitation. In oxygenic photoautotrophs, the number of Fe atoms is fourfold higher in PSI than in PSII (Table 1). Coincidentally, PSI reaction centres are about 24-fold more abundant than PSII in healthy *Trichodesmium* cells (Subramaniam *et al.*, 1999). This high PSI:PSII ratio may require higher levels of *psaA* expression than *psbA* (Fig. 3). But when iron is depleted, PSI undergoes a sharp decrease of reaction centre abundance (Fig. 1D), and a faster transcript degradation rate compared with PSII and Cyt b_{6f} (Fig. 4 and Table 2). This leads to a cascade of decreasing linear electron flow from PSII through Cyt b_{6f} to PSI (Fig. 5). This selective transition is extremely critical given the fact that *Trichodesmium* employs two antagonistic processes, oxygenic photosynthesis and oxygen-

sensitive nitrogen fixation, simultaneously during the photoperiod. Most cyanobacteria separate these two systems either spatially by localizing nitrogen fixation in specialized cells known as heterocysts (Wolk *et al.*, 1994), or temporally by fixing nitrogen at night at the expense of carbon reserves synthesized in the light (Bergman *et al.*, 1997). To protect nitrogenase, *Trichodesmium* must coordinate electron transport among different metabolic steps in photosynthesis, respiration and nitrogen fixation pathways (Scherer *et al.*, 1988). In effect, linear photosynthetic electron transport supplies electrons to reduce photosynthetically evolved O₂ via the Mehler reaction through PSI (Kana, 1992; 1993; Berman-Frank *et al.*, 2001b), and to stimulate carbohydrate synthesis for respiration; whereas cyclic electron flow provides adenosinetriphosphate (ATP) for N₂ fixation (Fig. 5). Second, a sequential progression directed at temporally separating the expression of nitrogenase, PSII and PSI over a diel cycle is enforced (Chen *et al.*, 1998; 1999). However, Fe deprivation exerts a profound burden upon PSI, which has an Fe demand secondary to nitrogenase and acts as an energy and reductant donor for nitrogenase. Moreover, iron stress results in an elevated level of reactive oxygen species (ROS) because several ROS-detoxifying enzymes, such as catalase, peroxidase or some superoxide dismutases, also require iron as a cofactor. The oxidative stress greatly affects the photosystems (Aro *et al.*, 1993; Bhaya *et al.*, 2000) and oxygen consumption by Mehler activity. Consequently, when fixed nitrogen is consumed and Fe cannot be compensated any more, nitrogen fixation ultimately becomes a prime target over the other metabolic pathways. This differential susceptibility is supported by the significantly lower rate of recovery of transcripts of *nifH* compared with photosynthetic genes (Table 2).

Our *in vivo* examination of Fe competition between the metabolic pathways appears to reflect the evolutionary history of photosynthesis and N₂ fixation in cyanobacteria and the oxidation state of the ocean on geological times (Falkowski *et al.*, 1998). Nitrogenase is an ancient biochemical innovation that almost certainly arose in the Archean Ocean before the oxidation of the atmosphere by oxygenic photoautotrophs (Falkowski, 1997; Zehr *et al.*, 2000). Under the prevailing anaerobic conditions of that period in Earth's history, Fe was relatively abundant in the upper ocean and N₂ was a readily available electron acceptor for anaerobic heterotrophic metabolism (Berman-Frank *et al.*, 2001b; 2003). In the contemporary ocean, oxygenic photosynthesis by cyanobacteria ultimately led to the oxidation of the atmosphere and oceans and to subsequent precipitation of Fe; hence, selection pressure has been directed on the evolution of the development of mechanisms to cope with a reduced bioavailability of iron. Marine non-heterocystous cyanobacteria, such as *Trichodesmium*, were strongly selected against

due to the hierarchy in the trade-off of metabolic pathways that require Fe. Nitrogen fixation appears to be one of the first pathways to be sacrificed in the cell.

Experimental procedures

Culture and growth conditions

Cultures of *T. erythraeum* IMS101 were grown in 1 l polycarbonate bottles at 26°C with constant aeration on a 12:12 h light/dark cycle at 100 µmol quanta m⁻² s⁻¹ in YBCII media (Chen *et al.*, 1996). Cultures were verified as axenic by staining with DAPI (4',6-diamidino-2-phenylindole) and visualizing under an epifluorescent microscope (Carl Zeiss, Thornwood, NY). To examine the development of iron deficiency, cells were grown to exponential phase in an iron-sufficient (+Fe) medium, with 0.4 µM FeCl₃ complexed with 2.0 µM EDTA. Equivalent biomass was then gently filtered onto 10 µm pore size polycarbonate filters (Osmonics, Minnetonka, MN), washed three times with media without added iron, and re-suspended in parallel cultures with or without Fe respectively. To restrict carryover Fe from the inoculum, the EDTA concentration was held at 2.0 µM in both conditions. Growth and pigment composition were monitored for 6 days following the transition. As pigmentation in the Fe-deficient (-Fe) culture declined (usually on day 3), a fraction of the iron-deficient cells was then transferred back to an iron-sufficient medium to demonstrate the ability of the cells to recover after short-term iron deficiency.

Pigment contents, absorption spectra and 77K fluorescence emission spectra

The chlorophyll *a* content was measured spectrophotometrically from methanol extracts (Mackinney, 1941). Absorption spectra of intact *Trichodesmium* cells were recorded with a DW-2000 UV-VIS spectrophotometer (SLM-AMINCO, Rochester, NY). Low temperature (77K) chlorophyll fluorescence emission measurements were obtained on cells flash frozen in a fibre optic-based liquid nitrogen Dewar attached to an AMINCO-BOWMAN Series 2 luminescence spectrometer (SLM-AMINCO). Cells were dark adapted at 25°C for 30 min before the low temperature measurements. Chlorophyll fluorescence was excited at 435 nm. Exciting and measuring slits were 4 nm. Corrected fluorescence emission spectra were recorded from 650 nm to 750 nm.

Variable fluorescence and photosynthetic parameters

Variable fluorescence was measured with a custom-built fast repetition rate fluorometer (FRRF), which measures fluorescence transients induced by a series of subsaturating excitation pulses from a bank of light emitting diodes (LEDs) to derive photosynthetic parameters (Kolber *et al.*, 1998). The photochemical quantum yield (F_v/F_m) was determined from the initial, dark-adapted fluorescence (F_o) and the maximal fluorescence (F_m) when all PSII reaction centres are photochemically reduced [$F_v/F_m = (F_m - F_o)/F_m$]. The functional absorption cross-section of PSII (σ_{PSII}), and changes in the reoxidation rate (τ) of the primary electron acceptor in PSII, quinone A (Q_A⁻), were calculated from the kinetics of fluorescence transients.

Target gene	Primer/probe	Sequence (5'-3')
<i>nifH</i>	nifH-682F	CAATACGCTCCAGAAGATAACCAA
	Reporter nifH-767R	CTTTTGAGCTAATTGATCG GTAGGAATAGTTAGTTTTTCGTTGTTGATT
<i>apcA</i>	apcA-56F	GTCCCGGTGAATTAGAGAGAATCAA
	Reporter apcA-122R	CAGCCTTGACAAAGTC TGAGCAATCCTAACACGGGTTTC
<i>psbA</i>	psbA-927F	CAGCGGTGCGTAATCAAT
	Reporter psbA-984R	CTTGGGCAGATATC CATTCTAAGTTAGCGCGTTAA
<i>psbE</i>	psbE-144F	CGGTACACCTCGACCTAATGAGTAT
	Reporter psbE-217R	ACTGAACAAAGACAAGAATTA ACTCAAAACGGTCTGACAAAATTGG
<i>psaA</i>	psaA-1046F	CCTGGCAGCCAGTTA
	Reporter psaA-1106R	CATAGCCAAGTTAATTGC GCCACAATGATGCTAAGAGATCCTA
<i>psaC</i>	psaC-109F	GGTCAAATTGCTTCATCTCCTCGTA
	Reporter psaC-180R	CAACGCTTACAACCAATACA CAGTAGGGCAAGCAGTCTCA
<i>petB</i>	petB-473F	TGTCTGGTGTACCTGATGCAATTC
	Reporter petB-541R	ATGAATGGACCAACAAATG TTGTACTACCACGCATCAGTTCTAC
<i>petC</i>	petC-243F	CCAAGGACTTAAAGGAGACCCTACT
	Reporter petC-339R	ATTCAGCCAAGGTTTGCTC ACACCCTAGATGAGTACATACTGCAT
<i>idiA</i>	idiA-651F	TGCGGCTGGCATTGGT
	Reporter idiA-716R	TTGGTCTTGCCAATAGCT GAAGATCTTTCAAACGCGCTAAGT
<i>isiA</i>	isiA-841F	GGAATTACTCCTTATTTTGCCGACAGT
	Reporter isiA-909R	CACCATTAGGCAACTTGA CAACCAACAACGAGCAGTATGAG
<i>mnpB</i>	mnpB-337F	TGGTAACAGGCATCCAGATAGATA
	Reporter mnpB-402R	CTGCCCTCAAAGCTTGT CGGGTTCTGTCTCTCAACTCAA

Table 3. Primers and probes used in this study for real-time RT-PCR.

Nitrogenase activity

Nitrogen fixation rates for *Trichodesmium* were measured using the acetylene reduction method (Capone, 1993). Aliquots (15 ml) were sealed in serum bottles, injected with purified acetylene (20% of headspace volume) and incubated at growth irradiance and temperature. Ethylene production was measured on an SRI 310 gas chromatograph (SRI Instruments, Torrance, CA) with a flame ionization detector at 0.5 h intervals for 2 h. The ethylene production rate was quantified relative to an ethylene standard and normalized to chlorophyll *a*. Sampling for nitrogenase activity was performed at the midpoint in the light cycle, when nitrogenase activity is maximal.

RNA sampling and extraction

At designated times, 50 ml samples of each culture type were removed and gravity filtered onto 5 µm-pore-size polycarbonate membrane filters (Osmonics). The filters were immediately frozen in liquid nitrogen and stored at -80°C until processing. Cells were sonicated with an ultrasonic cell disruptor (Misonix Microson) for 20 s on ice in 500 µl of RLT lysis buffer (Qiagen, Valencia, CA) and 7.5 µl of β-mercaptoethanol. The lysate was extracted using RNeasy spun columns (Qiagen) as recommended by the manufacturer. For real-time PCR analysis, DNA was removed by

15 min of DNase I digestion on the RNeasy columns with RNase-free DNase I from Qiagen. Total RNA was quantified spectrometrically and visualized with agarose gel electrophoresis before amplification by RT-PCR.

Real-time quantitative RT-PCR and Taqman assay

For quantitative RT-PCR assays, total RNA was reverse transcribed using a high-capacity cDNA archive Kit (Applied Biosystems, Foster City, CA) for the first-strand cDNA synthesis by following the manufacturer's specifications. The cDNA reaction mixtures consisted of 1 µg of total RNA, 2.5 µM random hexamers, 4 mM of each deoxynucleoside triphosphate (dNTP), 1× RT buffer, 5 mM MgCl₂ and 2.5 U MultiScribe Reverse Transcriptase. Negative control reactions without reverse transcriptase were run in parallel to ensure that there was no contaminating DNA and that the resulting amplification resulted from cDNA synthesis. Samples were reverse transcribed at 25°C for 10 min followed by 37°C for 120 min. The total reaction mixture volume was 100 µl and the cDNA was stored at -20°C until it was utilized in quantitative PCR assays.

To quantify the expression of the major iron-binding protein genes in both photosynthesis and nitrogen fixation apparatus, we designed PCR primers and TaqMan MGB probes (Table 3) with Primer Express software (Applied Biosystems). The targets include genes that encode nitrogenase iron protein (*nifH*), phycocyanin α-subunit (*apcA*), PSII reaction

centre D1 protein (*psbA*) and cytochrome *c*₅₅₉ α -subunit (*psbE*), PSI reaction centre apoprotein A1 (*psaA*) and iron-sulfur protein (*psaC*), and Cyt *b*₆*f* complex component Cyt *b*₆ (*petB*) and Rieske iron-sulfur subunit (*petC*). We also designed primers and probes to quantify the expression of the two iron stress-related protein-encoding genes, *idiA* and *isiA* (Table 3). The probe was labelled with the fluorescent reporter FAM (6-carboxyfluorescein) at 5' and non-fluorescent quencher at 3'.

Quantitative PCR was performed with triplicate 25 μ l of quantitative PCR mixtures for each sample. The reaction mixtures contained the equivalent of 5 ng of RNA (typically 11.25 μ l of diluted cDNA reaction mixture) as a template mixed with 1 \times TaqMan PCR buffer (Applied Biosystems), 0.25 U of AmpErase uracyl *N*-glycosylase (Applied Biosystems), 2.0 mM MgCl₂, 200 μ M (each) dATP, dGTP and dCTP, 400 μ M dUTP, 900 nM (each) TaqMan forward and reverse primers, 250 nM fluorogenic probe and 0.625 U AmpliTaq Gold DNA polymerase (Applied Biosystems). A GeneAmp 7900 sequence detection system (Applied Biosystems) was used for quantitative detection of amplified PCR products using the following thermal cycling conditions: 50°C for 2 min, 95°C for 10 min, and 40 cycles of 95°C for 15 s, followed by 60°C for 1 min.

The relative change in gene expression was endogenously normalized to the housekeeping gene *mpb*, encoding RNase P, calculated using the $2^{-\Delta\Delta Ct}$ method (Livak and Schmittgen, 2001) with the ΔCt (Ct, target gene – Ct, *mpb*) of the time zero Fe-sufficient control used as the calibrator. Ct is the threshold cycle for amplification of target genes or *mpb* from –Fe or +Fe cultures. The validity of using the $2^{-\Delta\Delta Ct}$ method was examined to ensure that the amplification efficiencies of the target genes and endogenous control *mpb* are approximately equal across the range of cDNA concentrations. To counter-balance effects of circadian gene expression (Chen *et al.*, 1998), we measured the transcript abundance at the same time each day in a time series experiment. The normalized data of transcript abundances were subjected to exponential regression analysis to estimate apparent half-lives, effective degradation rates and effective recovery rates. The differential gene expression was evaluated by *t*-test to determine statistical significance (at $P < 0.05$).

Acknowledgements

We thank John Waterbury and Eric Webb for graciously providing axenic cultures of *T. erythraeum* IMS 101, Donald Bryant, Oscar Schofield, Yibu Chen and Maxim Gorbunov for helpful discussions, and Kevin Wyman and Liti Haramaty for laboratory assistance. We also thank the anonymous reviewers who provided constructive comments that appreciably improve the manuscript. This work is supported by NASA through an interdisciplinary study grant Natural Iron Fertilization in the Ocean and Its Impacts on Ocean Nitrogen Fixation and Carbon Cycles (NNG04G091G) to P.G.F.

References

Aro, E.-M., Virgin, I., and Andersson, B. (1993) Photoinhibition of photosystem II. Inactivation, protein damage and

- turnover. *Biochim Biophys Acta (BBA) – Bioenergetics* **1143**: 113–134.
- Behrenfeld, M.J., Bale, A.J., Kolber, Z.S., Aiken, J., and Falkowski, P.G. (1996) Confirmation of iron limitation of phytoplankton photosynthesis in the equatorial Pacific Ocean. *Nature* **383**: 508–511.
- Behrenfeld, M.J., Worthington, K., Sherrell, R.M., Chavez, F.P., Strutton, P., McPhaden, M., and Shea, D.M. (2006) Controls on tropical Pacific Ocean productivity revealed through nutrient stress diagnostics. *Nature* **442**: 1025–1028.
- Bergman, B., Gallon, J.R., Rai, A.N., and Stal, L.J. (1997) N₂ fixation by non-heterocystous cyanobacteria. *FEMS Microbiol Rev* **19**: 139–185.
- Berman-Frank, I., Cullen, J.T., Shaked, Y., Sherrell, R.M., and Falkowski, P.G. (2001a) Iron availability, cellular iron quotas, and nitrogen fixation in *Trichodesmium*. *Limnol Oceanogr* **46**: 1249–1260.
- Berman-Frank, I., Lundgren, P., Chen, Y.-B., Küpper, H., Kolber, Z., Bergman, B., and Falkowski, P. (2001b) Segregation of nitrogen fixation and oxygenic photosynthesis in the marine cyanobacterium *Trichodesmium*. *Science* **294**: 1534–1537.
- Berman-Frank, I., Lundgren, P., and Falkowski, P. (2003) Nitrogen fixation and photosynthetic oxygen evolution in cyanobacteria. *Res Microbiol* **154**: 157–164.
- Berman-Frank, I., Bidle, K.D., Haramaty, L., and Falkowski, P.G. (2004) The demise of the marine cyanobacterium, *Trichodesmium* spp., via an autocatalyzed cell death pathway. *Limnol Oceanogr* **49**: 997–1005.
- Bhaya, D., Schwarz, R., and Grossman, A.R. (2000) Molecular responses to environmental stress. In *The Ecology of Cyanobacteria: Their Diversity in Time and Space*. Whitton, B.A., and Potts, M. (eds). Dordrecht, the Netherlands: Kluwer Academic Publishers, pp. 397–442.
- Bibby, T.S., Nield, J., and Barber, J. (2001) Iron deficiency induces the formation of an antenna ring around trimeric photosystem I in cyanobacteria. *Nature* **412**: 743–745.
- Boekema, E.J., Hifney, A., Yakushevskaya, A.E., Piotrowski, M., Keegstra, W., Berry, S., *et al.* (2001) A giant chlorophyll–protein complex induced by iron deficiency in cyanobacteria. *Nature* **412**: 745–748.
- Boyd, P.W., Jickells, T., Law, C.S., Blain, S., Boyle, E.A., Buesseler, K.O., *et al.* (2007) Mesoscale iron enrichment experiments 1993–2005: synthesis and future directions. *Science* **315**: 612–617.
- Braun, V., Schäffer, S., Hantke, K., and Tröger, W. (1990) Regulation of gene expression by iron. In *The Molecular Basis of Bacterial Metabolism*. Hauska, G., and Thauer, R. (eds). New York, USA: Springer, pp. 164–179.
- Burnap, R.L., Troyan, T., and Sherman, L.A. (1993) The highly abundant chlorophyll–protein complex of iron-deficient *Synechococcus* sp. PCC7942 (CP43') is encoded by the *isiA* gene. *Plant Physiol* **103**: 893–902.
- Capone, D.G. (1993) Determination of nitrogenase activity in aquatic samples using the acetylene reduction procedure. In *Handbook of Methods in Aquatic Microbial Ecology*. Kemp, P.F., Sherr, B.F., Sherr, E.B., and Cole, J.J. (eds). Boca Raton, FA, USA: Lewis Press, pp. 621–631.
- Capone, D.G., Zehr, J.P., Paerl, H., Bergman, B., and Carpenter, E.J. (1997) *Trichodesmium*, a globally

- significant marine cyanobacterium. *Science* **276**: 1221–1229.
- Carpenter, E.J. (1983) Nitrogen fixation by marine *Oscillatoria* (*Trichodesmium*) in the world's oceans. In *Nitrogen in the Marine Environment*. Carpenter, E.J., and Capone, D.G. (eds). New York, USA: Academic Press, pp. 65–103.
- Chen, Y.-B., Zehr, J.P., and Mellon, M. (1996) Growth and nitrogen fixation of the diazotrophic filamentous nonheterocystous cyanobacterium *Trichodesmium* sp. IMS101 in defined media: evidence for a circadian rhythm. *J Phycol* **32**: 916–923.
- Chen, Y.-B., Dominic, B., Mellon, M.T., and Zehr, J.P. (1998) Circadian rhythm of nitrogenase gene expression in the diazotrophic filamentous nonheterocystous cyanobacterium *Trichodesmium* sp. strain IMS 101. *J Bacteriol* **180**: 3598–3605.
- Chen, Y.-B., Dominic, B., Zani, S., Mellon, M.T., and Zehr, J.P. (1999) Expression of photosynthesis genes in relation to nitrogen fixation in the diazotrophic filamentous nonheterocystous cyanobacterium *Trichodesmium* sp. IMS 101. *Plant Mol Biol* **41**: 89–104.
- Cody, G.D., Boctor, N.Z., Filley, T.R., Hazen, R.M., Scott, J.H., Sharma, A., and Yoder, H.S., Jr (2000) Primordial carbonylated iron-sulfur compounds and the synthesis of pyruvate. *Science* **289**: 1337–1340.
- Davis, C.S., and McGillicuddy, D.J., Jr (2006) Transatlantic abundance of the N₂-fixing colonial cyanobacterium *Trichodesmium*. *Science* **312**: 1517–1520.
- Duce, R.A., and Tindale, N.W. (1991) Atmospheric transport of iron and its deposition in the ocean. *Limnol Oceanogr* **36**: 1715–1726.
- Durnford, D.G., and Falkowski, P.G. (1997) Chloroplast redox regulation of nuclear gene transcription during photoacclimation. *Photosynth Res* **53**: 229–241.
- Escoubas, J., Lomas, M., LaRoche, J., and Falkowski, P.G. (1995) Light intensity regulation of cab gene transcription is signaled by the redox state of the plastoquinone pool. *Proc Natl Acad Sci USA* **92**: 10237–10241.
- Falkowski, P.G. (1997) Evolution of the nitrogen cycle and its influence on the biological sequestration of CO₂ in the ocean. *Nature* **387**: 272–275.
- Falkowski, P.G., Barber, R.T., and Smetacek, V. (1998) Biogeochemical controls and feedbacks on ocean primary production. *Science* **281**: 200–206.
- Ferreira, F., and Straus, N.A. (1994) Iron deprivation in cyanobacteria. *J Appl Phycol* **6**: 199–210.
- Ferreira, K.N., Iverson, T.M., Maghlaoui, K., Barber, J., and Iwata, S. (2004) Architecture of the photosynthetic oxygen-evolving center. *Science* **303**: 1831–1838.
- Gao, Y., Kaufman, Y.J., Tanre, D., Kolber, D., and Falkowski, P.G. (2001) Seasonal distributions of aeolian iron fluxes to the global ocean. *Geophys Res Lett* **28**: 29–32.
- Geider, R.J., and La Roche, J. (1994) The role of iron in phytoplankton photosynthesis, and the potential for iron-limitation of primary productivity in the sea. *Photosynth Res* **39**: 275–301.
- Ghassemian, M., and Straus, N. (1996) Fur regulates the expression of iron-stress genes in the cyanobacterium *Synechococcus* sp. strain PCC 7942. *Microbiology* **142**: 1469–1476.
- Greene, R.M., Geider, R.J., and Falkowski, P.G. (1991) Effect of iron limitation on photosynthesis in a marine diatom. *Limnol Oceanogr* **36**: 1772–1782.
- Guikema, J.A., and Sherman, L.A. (1983) Organization and function of chlorophyll in membranes of cyanobacteria during iron starvation. *Plant Physiol* **73**: 250–256.
- Ivanov, A.G., Park, Y.-I., Miskiewicz, E., Raven, J.A., Huner, N.P.A., and Oquist, G. (2000) Iron stress restricts photosynthetic intersystem electron transport in *Synechococcus* sp. PCC 7942. *FEBS Lett* **485**: 173–177.
- Jordan, P., Fromme, P., Witt, H.T., Klukas, O., Saenger, W., and Krauß, N. (2001) Three-dimensional structure of cyanobacterial photosystem I at 2.5 Å resolution. *Nature* **411**: 909–917.
- Kana, T.M. (1992) Relationship between photosynthetic oxygen cycling and carbon assimilation in *Synechococcus* WH7803 (Cyanophyta). *J Phycol* **28**: 304–308.
- Kana, T.M. (1993) Rapid oxygen cycling in *Trichodesmium thiebautii*. *Limnol Oceanogr* **38**: 18–24.
- Karl, D., Letelier, R., Tupas, L., Dore, J., Christian, J., and Hebel, D. (1997) The role of nitrogen fixation in biogeochemical cycling in the subtropical North Pacific Ocean. *Nature* **388**: 533–538.
- Kolber, Z.S., Prasil, O., and Falkowski, P.G. (1998) Measurements of variable chlorophyll fluorescence using fast repetition rate techniques: defining methodology and experimental protocols. *Biochim Biophys Acta (BBA) – Bioenergetics* **1367**: 88–106.
- Kurisu, G., Zhang, H., Smith, J.L., and Cramer, W.A. (2003) Structure of the cytochrome *b₆f* complex of oxygenic photosynthesis: tuning the cavity. *Science* **302**: 1009–1014.
- Kustka, A., Sañudo-Wilhelmy, S., Carpenter, E.J., Capone, D.G., and Raven, J.A. (2003a) A revised estimate of the iron use efficiency of nitrogen fixation, with special reference to the marine cyanobacterium *Trichodesmium* spp. (Cyanophyta). *J Phycol* **39**: 12–25.
- Kustka, A.B., Sañudo-Wilhelmy, S.A., Carpenter, E.J., Capone, D., Burns, J., and Sunda, W.G. (2003b) Iron requirements for dinitrogen- and ammonium-supported growth in cultures of *Trichodesmium* (IMS 101): comparison with nitrogen fixation rates and iron: carbon ratios of field populations. *Limnol Oceanogr* **48**: 1869–1884.
- Lax, J.E.-M., Arteni, A.A., Boekema, E.J., Pistorius, E.K., Michel, K.-P., and Rögner, M. (2007) Structural response of Photosystem 2 to iron deficiency: characterization of a new Photosystem 2-IdiA complex from the cyanobacterium *Thermosynechococcus elongatus* BP-1. *Biochimica et Biophysica Acta (BBA)-Bioenergetics* **1767**: 528–534.
- Livak, K.J., and Schmittgen, T.D. (2001) Analysis of relative gene expression data using real-time quantitative PCR and the 2^{-ΔΔC_t} method. *Methods* **25**: 402–408.
- Lundgren, P., Janson, S., Jonasson, S., Singer, A., and Bergman, B. (2005) Unveiling of novel radiations within *Trichodesmium* cluster by *hetR* gene sequence analysis. *Appl Environ Microbiol* **71**: 190–196.
- Mackinney, G. (1941) Absorption of light by chlorophyll solution. *J Biol Chem* **140**: 315–322.
- Martin, J.H., Coale, K.H., Johnson, K.S., Fitzwater, S.E., Gordon, R.M., Tanner, S.J., et al. (1994) Testing the iron hypothesis in ecosystems of the equatorial Pacific Ocean. *Nature* **371**: 123–129.
- Michel, K.-P., and Pistorius, E.K. (2004) Adaptation of the

- photosynthetic electron transport chain in cyanobacteria to iron deficiency: the function of *IdiA* and *IsiA*. *Physiol Plantarum* **120**: 36–50.
- Michel, K., Thole, H., and Pistorius, E. (1996) *IdiA*, a 34 kDa protein in the cyanobacteria *Synechococcus* sp. strains PCC 6301 and PCC 7942, is required for growth under iron and manganese limitations. *Microbiology* **142**: 2635–2645.
- Morel, F.M.M., Rueter, J.G., and Price, N.M. (1991) Iron nutrition of phytoplankton and its possible importance in the ecology of ocean regions with high nutrient and low biomass. *Oceanography* **4**: 56–61.
- Öquist, G. (1974) Iron deficiency in the blue-green alga *Anacystis nidulans*: fluorescence and absorption spectra recorded at 77K. *Physiol Plantarum* **31**: 55–58.
- Paerl, H.W. (1994) Spatial segregation of CO₂ fixation in *Trichodesmium* sp.: linkage to N₂ fixation potential. *J Phycol* **30**: 790–799.
- Pakrasi, H.B., Riethman, H.C., and Sherman, L.A. (1985) Organization of pigment proteins in the photosystem II complex of the cyanobacterium *Anacystis nidulans* R2. *Proc Natl Acad Sci USA* **82**: 6903–6907.
- Park, Y.-I., Sandström, S., Gustafsson, P., and Öquist, G. (1999) Expression of the *isiA* gene is essential for the survival of the cyanobacterium *Synechococcus* sp. PCC 7942 by protecting photosystem II from excess light under iron limitation. *Mol Microbiol* **32**: 123–129.
- Raven, J.A. (1988) The iron and molybdenum use efficiencies of plant growth with different energy, carbon and nitrogen sources. *New Phytol* **109**: 279–287.
- Raven, J.A. (1990) Predictions of Mn and Fe use efficiencies of phototrophic growth as a function of light availability for growth and of C assimilation pathway. *New Phytol* **116**: 1–18.
- Rueter, J.G., Ohki, K., and Fujita, Y. (1990) The effect of iron nutrition on photosynthesis and nitrogen fixation in cultures of *Trichodesmium* (Cyanophyceae). *J Phycol* **26**: 30–35.
- Rueter, J.G., Hutchins, D.A., Smith, R.W., and Unsworth, N.L. (1992) Iron nutrition of *Trichodesmium*: establishment of culture and characteristics of N₂-fixation. In *Marine Pelagic Cyanobacteria: Trichodesmium and Other Diazotrophs*. Carpenter, E.J., Capone, D.G., and Rueter, J.G. (eds). Dordrecht, the Netherlands: Kluwer Academic Publishers, pp. 289–306.
- Sandström, S., Ivanov, A.G., Park, Y.-I., Öquist, G., and Gustafsson, P. (2002) Iron stress responses in the cyanobacterium *Synechococcus* sp. PCC7942. *Physiol Plantarum* **116**: 255–263.
- Scherer, S., Almon, H., and Böger, P. (1988) Interaction of photosynthesis, respiration and nitrogen fixation in cyanobacteria. *Photosynth Res* **15**: 95–114.
- Schindelin, H., Kisker, C., Schlessman, J.L., Howard, J.B., and Rees, D.C. (1997) Structure of ADP•AlF₄⁻-stabilized nitrogenase complex and its implications for signal transduction. *Nature* **387**: 370–376.
- Shi, T., Bibby, T.S., Jiang, L., Irwin, A.J., and Falkowski, P.G. (2005) Protein interactions limit the rate of evolution of photosynthetic genes in cyanobacteria. *Mol Biol Evol* **22**: 2179–2189.
- Straus, N.A. (1994) Iron deprivation: physiology and gene regulation. In *The Molecular Biology of Cyanobacteria*. Bryant, D.A. (ed.). Dordrecht, the Netherlands: Kluwer Academic Publishers, pp. 731–750.
- Subramaniam, A., Carpenter, E.J., Karentz, D., and Falkowski, P.G. (1999) Bio-optical properties of the marine diazotrophic cyanobacteria *Trichodesmium* spp. I. Absorption and photosynthetic action spectra. *Limnol Oceanogr* **44**: 608–617.
- Webb, E.A., Moffett, J.W., and Waterbury, J.B. (2001) Iron stress in open-ocean cyanobacteria (*Synechococcus*, *Trichodesmium*, and *Crocospaera* spp.): identification of the *IdiA* protein. *Appl Environ Microbiol* **67**: 5444–5452.
- Westberry, T.K., and Siegel, D.A. (2006) Spatial and temporal distribution of *Trichodesmium* blooms in the world's oceans. *Global Biogeochem Cycles* **20**: 1–13.
- Wolk, C.P., Ernst, A., and Elhai, J. (1994) Heterocyst metabolism and development. In *The Molecular Biology of Cyanobacteria*. Bryant, D.A. (ed.). Dordrecht, the Netherlands: Kluwer Academic, pp. 769–823.
- Yousef, N., Pistorius, E.K., and Michel, K.-P. (2003) Comparative analysis of *idiA* and *isiA* transcription under iron starvation and oxidative stress in *Synechococcus elongatus* PCC 7942 wild-type and selected mutants. *Arch Microbiol* **180**: 471–483.
- Zehr, J.P., Carpenter, E.J., and Villareal, T.A. (2000) New perspectives on nitrogen-fixing microorganisms in tropical and subtropical oceans. *Trends Microbiol* **8**: 68–73.
- Zehr, J.P., Waterbury, J.B., Turner, P.J., Montoya, J.P., Omeregic, E., Steward, G.F., et al. (2001) Unicellular cyanobacteria fix N₂ in the subtropical North Pacific Ocean. *Nature* **412**: 635–638.